Submitted to
Physical Review

LBL-1313
Preprint

ELECTRON AVALANCHE IN LIQUID XENON

Stephen E. Derenzo, Terry S. Mast, and Haim Zaklad
and Richard A. Muller

March 1973

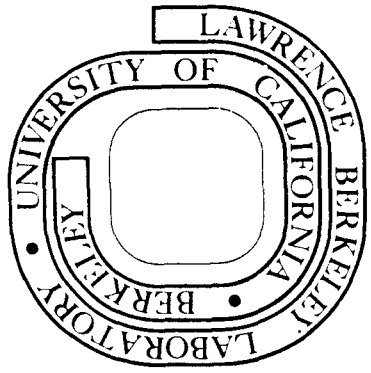

Prepared for the U. S. Atomic Energy Commission
under Contract W-7405-ENG-48

ELECTRON AVALANCHE IN LIQUID XENON*

Stephen E. Derenzo, Terry S. Mast, and Haim Zaklad
Lawrence Berkeley Laboratory, University of California
Berkeley, California 94720
and
Richard A. Muller, Space Science Laboratory, University of California
Berkeley, California 94720

March 1973

ABSTRACT

We present detailed measurements of the electron avalanche process in liquid Xenon. The measurements were made by using liquid-Xe-filled proportional chambers with anode diameters of 2.9, 3.5, and 5.0 μ to detect 279-keV γ rays and measure the photopeak pulse height as a function of applied voltage. The use of uniform pulses of electrons enabled us to discriminate against secondary Townsend processes. We present a table of the first Townsend coefficient α as a function of electric field E; a typical value is $\alpha = (4.5\pm0.3) \times 10^4$ cm^{-1} at $E = 2 \times 10^6$ V/cm. The electron avalanche occurs in liquid Xe at electric fields 26 times smaller than would be predicted using measurements made in gaseous Xe and E/ρ density scaling.

I. INTRODUCTION

It has been known for over two decades that excess electrons (such as those freed by the passage of ionizing radiation) in very pure liquified Ar and Xe remain free and have high mobility in applied electric fields.[1-5] These mobility data have been successfully interpreted in terms of gas kinetic theory, implying that electrons move in these liquids as they would in compressed gases.[6,7]

In 1968 Alvarez suggested[8] that the noble liquids might have important applications for high-energy nuclear particle detection, particularly if the electronic signal could be increased by inducing an electron avalanche in the liquid (similar to that which occurs in gas-filled detectors). By using suitably high electric fields we were able to induce electron avalanche in both liquid Ar and liquid Xe.[9-11] Only in liquid Xe did we observe a "well behaved" avalanche (i.e., one which had characteristics similar to those of a gaseous avalanche).[12] In this paper we report measurements in liquid Xe of the characteristic function that describes the avalanche, the first Townsend coefficient.

Electron avalanche occurs when the drifting electrons attain sufficient kinetic energy from the electric field to cause additional ionization. The first Townsend coefficient α is defined by the equation

$$dQ = \alpha Q\, dr, \tag{1.1}$$

where dQ is the charge of electrons (and Xe^+ ions) liberated in the avalanche when an electron charge Q drifts through a distance dr; α can be a function of electric field, density, temperature, pressure, and the other parameters of the gas or liquid. In our experiments the only such parameter that varied by a significant amount was the electric field E. We obtained data on the avalanche by studying the pulses in a liquid-

filled proportional chamber as a function of applied voltage and anode diameter. Preliminary results were reported previously.[10]

II. DESCRIPTION OF THE EXPERIMENT

The experimental apparatus, a single-wire proportional chamber, is shown in Fig. 1. The chamber cathode was 8 mm in diameter and 30 mm long, formed by depositing a conductive coating of SnO on the cylindrical inside glass wall of the chamber. The anode was a fine tungsten wire, alternately 2.9, 3.5, or 5.0 μ in diameter.[13] The wires were tensioned at 60% of their breaking load and soldered to feed-throughs at the top and bottom of the chamber. Several samples of each wire were photographed with a scanning electron microscope that was calibrated with a Buckbee-Meers screen[14] having 2000 meshes per inch (see Fig. 2). Variations in wire diameter were typically ±1.5%. To drive contaminants from the chamber walls, the chamber was kept at a temperature of 100°C and an internal pressure below 10^{-6} Torr for a period of at least 15 hours prior to filling. The chamber was filled with Xe gas from a specially designed noble gas purifier[15] and then cooled to -107°C (the boiling point of liquid Xe) by immersion in a thermostatically controlled bath of Freon-11 ($FCCl_3$). Although our purifier reliably delivers Xe gas that contains <50 ppb of O_2 and <100 ppb of either N_2, CO_2, or CH_4, the chamber fills with a liquid that typically contains electronegative impurities (as yet unidentified) equivalent in electron capture ability to several ppm O_2. (See Ref. 15 for details.) Difficulty in removing electronegative impurities from liquid Xe has been mentioned by other workers.[16,17] We are able to eliminate almost all of these electronegative impurities by using field emission electrons to sweep them to the outer electrode. A potential of approximately 5 kV is applied to the outer electrode, causing

the fine central wire to emit (typically) 5μA of current. After 10 min of this electronegative ion pumping the pulse height reaches a level that is not increased by further processing. (It may be readily calculated that < 300 ppb of impurities are removed.) Re-processing is required only after a period of several hours. These techniques are capable of reducing the impurity level to the point where electrons have a mean free path >20cm, as measured in a parallel-plate ionization chamber with a Frisch grid.

A collimated ^{203}Hg source was used to send a 1.2-mm-diameter beam of 68-keV x-rays and 279 keV gamma rays into the 8-mm-diameter cylindrical chamber. The resulting recoil electron pulses were detected with a charge-sensitive amplifier of the type used for solid state detectors. Electronic filtering consisting of 1-μsec integration (risetime) and 5-μsec differentiation (fall time) was chosen to maximize the signal-to-noise ratio. With this filtering, the noise was equivalent to 1.2×10^{-16}C FWHM at the input of the charge-sensitive amplifier. The chamber capacitance was 4.5 pF. A typical pulse height distribution for the ^{203}Hg source (recorded on a RIDL model 34-12B pulse height analyzer) and shown in Fig. 3, clearly shows the photopeak and Compton edge for the 279-keV γ-ray and the photopeak for the 68-keV x ray. The pulse height of the 279 keV photopeak is shown in Fig. 4 as a function of applied voltage for 2.9, 3.5, and 5.0 μ diameter tungsten wires. The amplifiers and pulse-height analyzer were calibrated by injecting pulses of known voltage and 200-nsec risetime through a 10 pF capacitor directly into the charge sensitive amplifier.

III. INITIAL ANALYSIS

The data in Fig. 4 have the following qualitative interpretation: At the lowest voltages an appreciable fraction of the electrons recombine with Xe^+ ions before the electrons can contribute to the pulse. As the voltage is increased nearly all the electrons escape recombination, and the pulse height reaches a plateau. The height of this plateau varies by about 10% from run to run due to variations in the level of electronegative impurities or possible calibration errors. At higher voltages, the electrons avalanche in the high electric field near the anode, resulting in a rapid increase of pulse height with voltage. At our highest voltages the space charge of the slow Xe^+ ions reduces the field near the wire, causing a saturation of pulse height and a broadening of the photopeak. (We found that the saturation charge decreased by a factor 3 when the counting rate was increased from 200 to 2000 sec^{-1} by tripling the diameter of the collimator hole. The data in Fig. 4 were taken with a counting rate of 200 sec^{-1}).

At voltages slightly beyond those shown in Fig. 4, the photopeak is obscured by a large number of pulses (not related to the presence of the γ-ray source) of irregular shape and size. Investigation at higher voltages is prevented by the onset of sparking through the liquid at many places between the cathode and the anode wire. When the number of sparks exceeds $\sim 10^3$, the anode wire often breaks.

One estimate of the first Townsend coefficient may be obtained by comparing the pulse heights of two chambers having different-size wires but the same electric field function E(r) where r is the distance to the center of the wire. The ratio of these pulse heights will be the additional gain from the avalanche that occurs in the distance from the larger-wire radius to the smaller-wire radius.

For example, one obtains the same function E(r) (in the region $r \geq 1.75$ μ) for a 2.9-μ-diameter wire at 1800 volts as for a 3.5-μ-diameter wire at 1765 volts. From Fig. 4, we see that for the two wires at their respective voltages the pulse heights are 6.6 and 2.9 $\times 10^{-15}$C. As we expe the avalanche to be identical in the regions where the fields are identical, we conclude that the additional gain of 6.6/2.9 = 2.3 occurred during the last 0.3 μ of the avalanche, i.e., as the avalanche progressed from the virtual surface of the larger wire at r = 1.75 μ to the actual surface of the finer wire at r = 1.45 μ. Assuming that the ratio of the gains is equal to the ratio of the size of the avalanches, this implies an average first Townsend coefficient of $\alpha = \ln(2.3)/0.3\ \mu = 28\ 000\ cm^{-1}$. The electric field in this region varied from 1.29×10^6 to 1.57×10^6 V/cm.

In order to remove the equal-ratio assumption and to study the behavior of the first Townsend coefficient in detail, we made a simultaneous fit to all the data of Fig. 4 below 200 fC. We now consider the details of that fit.

IV. DETAILED ANALYSIS

TABLE I. Glossary

Q_o	Initial ionization in liquid produced by a 279 keV photoelectron.
Q_o'	Initial ionization reduced by electron capture processes that do not depend on the strength of the electric field.
$Q_1(r)$	Initial ionization escaping recombination.
$Q_2(r)$	Initial ionization escaping recombination and capture by impurities.
$Q_3(r,r')$	Amount of electron (and Xe^+ ion) charge produced in the avalanche as the electron charge $Q_2(r)$ drifts from r to r'.
Q_4	Charge induced at charge amplifier by motion of initial ionization electrons (averaged over all photoelectron positions r).
Q^-	Charge induced at charge amplifier by motion of avalanche electrons (averaged over all photoelectron positions).
$Q^+(T)$	Charge induced at charge amplifier by motion of avalanche Xe^+ ions during time T (averaged over all photoelectron positions).
K	Recombination coefficient.
λ	Coefficient of electron capture processes having a 1/E dependence.
r_1	Radius of anode wire.
r_2	Radius of cathode (4 mm for this experiment).
V	Anode-cathode potential.
E(r)	Strength of electric field.
T	Time during which charge motion can contribute to the pulse height at the output of the amplifier; determined by amplifier pulse shaping.

When a 279-keV γ ray produces a photoelectron in liquid Xe, the photoelectron is severely multiple Coulomb scattered in the liquid. It produces approximately 12 500 ion pairs distributed about the γ-ray interaction point within a distance of 240 μ.[18] We shall therefore consider each photoelectron to produce a point-like packet of initial ionization at some distance r from the central axis of the chamber. Since the beam of 279-keV γ rays was much narrower than the chamber (1.2 mm diam vs 8 mm diam) and attenuation was small, the distribution of values of r is fairly uniform. Consequently, after evaluating the expression for the pulse height as a function of photoelectron position r, initial ionization Q_o, recombination, electron attachment, and first Townsend coefficient we will average over all r.

The amount of electron charge Q_1 that escapes recombination may be approximated by

$$Q_1(r) = \frac{Q_o}{1 + K/E(r)}, \tag{4.1}$$

where $E(r) = V/[r\ln(r_2/r_1)]$, r is the radial coordinate of the γ-ray interaction point, Q_o is the initial ionization, E(r) is the electric field at the position of the photoelectron, and K is the "recombination coefficient. This formula was used by Marshall[4] and is based on the Jaffe theory.[19]

As the electron charge Q_1 drifts toward the center of the chamber, it is subject to capture by electronegative impurities. The amount of free electron charge Q_2 reaching the central region of the chamber is given by

$$Q_2(r) = Q_1(r) \exp\left[\int_{r_1}^{r} -\sigma(r)dr\right], \tag{4.2}$$

where r is the radial position of the photoelectron, r_1 is the anode radius, and σ is the probability of electron capture per cm of drift. Swan studied the dependence of σ on electric field (E) for small amounts of oxygen in liquid argon and found that $\sigma = (8 \times 10^{9}\ V/cm^{2})\ F/E$, where F is the fraction of oxygen.[7] Since we are dealing with unknown contaminants in liquid xenon (rather than oxygen in liquid argon) we choose to approximate $\sigma(r)$ by the more general formula

$$\sigma(r) = \sigma_0 + \lambda/E(r), \text{ where } \sigma_0 \text{ and } \lambda \text{ are appropriate positive constants} \qquad (4.3)$$

We can find the integrated electron capture by using the r^{-1} dependence of the electric field:

$$\int_{r_1}^{r} -\sigma(r)dr = -r\left[\sigma_o + \frac{\lambda}{2E(r)}\right], \qquad (4.4)$$

where we have neglected terms of order r_1/r. Substituting the evaluated integral into Eq. (4.2), we find

$$Q_2(r) = Q_o \exp(-r\sigma_o) \exp\left[-r\lambda/2E(r)\right] \Big/ \left[1 + K/E(r)\right]$$

$$= Q_o' \exp\left[-r\lambda/2E(r)\right] \Big/ \left[1 + K/E(r)\right], \qquad (4.5)$$

where we have absorbed into the coefficient Q_o' those electron attachment terms that do not depend on the electric field.

It can be seen in Fig. 4 that below the onset of avalanche (i.e., below 1200 V) the three experimental curves differ by multiplicative factors (between 0.9 and 1.1) and that these factors do not vary by any significant amount (<2%) from 100 to 1200 V. Consequently, Q_o' was allowed to take different values for each of the 2.9-, 3.5-, and 5.0-μ runs, while k and λ, parameters that control voltage-dependent factors,

were each required to take only a single value for all the data.

As the electron charge Q_2 approaches the fine central wire, it begins to avalanche. When the resulting electron swarm has reached distance r' from the center of the wire, its size is given by integrating Eq (1.1):

$$Q_3(r,r') = Q_2(r) \exp \int_{r}^{r'} \alpha(r'')\, dr''. \qquad (4.6)$$

The remaining analysis consists of calculating the charge induced at the anode by the motion of the ionization charge $Q_2(r)$ and the avalanche charge $Q_3(r, r')$.

In general, as a charge dq drops through a potential difference dV it induces a charge d^2Q on the anode given by[20]

$$d^2Q = dq\,\frac{dV}{V}. \qquad (4.7)$$

For a charge moving from r to r_f in a chamber of cylindrical geometry this becomes, after integration,

$$dQ = dq\,\frac{\ln(r/r_f)}{\ln(r_2/r_1)}. \qquad (4.8)$$

For small electron capture, the charge induced at the anode by the motion of the *initial ionization electrons* (averaging over all photoelectron positions) may be closely approximated by

$$Q_4 = \int_{r_1}^{r_2} \frac{Q_2(r)\ln(r/r_1)}{r_2\ln(r_2/r_1)}\, dr. \qquad (4.9)$$

The avalanche produces a pulse at the charge-sensitive amplifier due to the drift of the *avalanche electrons* toward the wire and by the drift of the *avalanche* Xe^+ *ions* away from the wire. The avalanche electrons drift at their saturated velocity [16] of 3×10^5 cm/sec and reach the surface of the anode in a few nanoseconds. On

the other hand the avalanche Xe^+ ions travel very slowly, requiring approximately 1 sec to drift from the anode to the cathode. Their mobility[21] is 3×10^{-4} cm^2 volt^{-1} sec.$^{-1}$ To have an acceptable signal-to-noise ratio, it is necessary to accept charge only during some small time interval T; i.e., to filter out the low-frequency noise components. Hence the filtered pulse from the amplifier is produced by the drift of the e^- and Xe^+ ions only during the time T. Our amplifier and filter (1-μsec integration, 5-μsec differentiation) responded to a charge impulse (of 10-nsec width) with an output pulse that peaked 1.8 μsec after the initial rise. The electron avalanche pulses peaked in 2.0 μsec and were thus in effect only slightly slower than instantaneous pulses.

For 10^{-7} sec < T < 10^{-1} sec the filtered pulse contains all of the avalanche e^- contribution but only a fraction of the Xe^+ contribution. It has been shown[22] that during a time T in a chamber of cylindrical geometry the Xe^+ ions produced in the avalanche will travel from r to r^+, given by

$$r^+ = \sqrt{r^2 + \frac{2\mu TV}{\ln(r_2/r_1)}}\ , \qquad (4.10)$$

where μ is the mobility of the Xe^+ ions, r_1 is the anode radius, and V is the potential on the chamber.

From Eq. (1.1), the additional electron (and Xe^+ ion) charge generated by the avalanche between r' and r' - dr' is given by

$$dQ_3(r, r') = Q_3(r, r')\alpha(r')dr'. \qquad (4.11)$$

To calculate the charge Q^- induced at the anode by all avalanche electrons we multiply Eq. (4.11) (the differential electron charge) by Eq. (4.8) (the charge fraction induced when electrons drift from r' to the anode at r_1), integrate over r' (to include the entire avalanche), and finally average over all photoelectron positions r:

$$Q^- = \int_{r_1}^{r_2}\int_{r_1}^{r_2} \frac{\ln(r'/r_1)}{r_2\ln(r_2/r_1)} Q_3(r,r')\alpha(r')dr'dr. \qquad (4.12)$$

To calculate the charge $Q^+(T)$ induced at the anode by all avalanche Xe^+ ions, we multiply Eq. (4.11) (the differential Xe^+ ion charge) by Eq. (4.8) (the charge fraction induced when Xe^+ ions drift outward for time T), integrate over r', and average over r:

$$Q^+(T) = \int_{r_1}^{r_2}\int_{r_1}^{r_2} \frac{\ln(r'/r^+)}{r_2\ln(r_2/r_1)} Q_3(r,r')\alpha(r')dr'dr. \qquad (4.13)$$

V. RESULTS IN LIQUID XENON

The sum of Eqs. (4.9), (4.12) and (4.13) were fitted to the data of Fig. 4 by adjusting the parameters Q_o', K, λ and nine independent values of α for E = 400 kV/cm to 2000 kV/cm in steps of 200 kV/cm. The integrals were computed numerically. The best fit values are shown in Table II. Although Q_o' was allowed to take a different value for each of the 2.9-, 3.5-, and 5.0-μ runs to allow for differences in the level of electronegative impurities and possible calibration errors, K, λ, and α(E) were required to fit the data for all three runs simultaneously. The fitting program used a linear interpolation on the table of log α vs E to define the function α(E) in Eq. (4.6). Since the pulses peaked 2 μsec after their rise, we fixed T at 2 μsec. When the fit was repeated assuming a value of 1.5 μsec for T, the best fit values of each parameter changed by less than 0.15 standard deviation. From measurements of the average ionization potential of gaseous Xe (21.9 eV/ion pair),[23] a 279-keV photoelectron should produce 2.04 X10^{-15}C of initial ionization (Q_o). We see from Table II that the average of the fitted values of Q_o' is only 3% smaller than the expected value of Q_o, indicating that the loss of

electrons to impurities was a minor effect. Moreover, the best fit value for λ, the field-dependent attachment coefficient, was zero with a one-standard-deviation upper limit of 10 V/cm^2. Swan found[7] that for 1 ppm O_2 in liquid argon, $\lambda = 8 \times 10^3$ V/cm^2.

We assigned a ±10% uncertainty to each experimental datum point and the χ^2 fit yielded the parameters shown in Table II. The data above 200 X10^{-15}C were omitted from the fit in order to exclude saturation effects. The resulting values of $\alpha(E)$ agree with those determined by the simple method described in Section III. The data for each rum are plotted in Fig. 5 with the curves from the fit, and the agreement is very good. The best fit χ^2 was 84.0 with 111 degrees of freedom, verifying the value of the uncertainty (±10%) assigned to the data.

In Fig. 6 we plot the pulse induced on the charge amplifier as a function of photoelectron position r for several voltages in the 2.9$^-$μ run. These curves are the sum of the integrands in Eqs. (4.9), (4.12), and (4.13), before the averaging over r.

In Fig. 7 we plot the total charge G produced in the avalanche, the charge G^- induced by the motion of the avalanche e^-, and the charge G^+ induced by the motion of the avalanche Xe^+ ions during the first 2 μsec as a function of voltage for the 2.9- and 5.0-μ wires. These three curves are based on the parameters shown in Table II and normalized to one initial electron.

For this calculation, we define:

$$G = \exp \int_{r_1}^{r_2} \alpha(r'')\, dr'', \tag{5.1}$$

$$G^- = \int_{r_1}^{r_2} \frac{\ln (r'/r_1)}{\ln (r_2/r_1)} \left[\exp \int_{r'}^{r_2} \alpha(r'')dr'' \right] \alpha(r')dr', \tag{5.2}$$

$$G^+ = \int_{r_1}^{r_2} \frac{\ln(r^+/r')}{\ln(r_2/r_1)} \left[\exp \int_{r'}^{r_2} \alpha(r'')dr'' \right] \alpha(r')dr' . \tag{5.3}$$

We see that of the charge produced in the avalanche (G) only a small fraction ($G^- + G^+$) is actually observed. This fraction varied from 0.10 to 0.19 during this experiment, increasing either with increasing voltage or with decreasing wire diameter. This behavior is quite reasonable, since an increase in the field at the anode causes the Xe^+ ions to travel a greater distance per microsecond. Fig. 7 also shows that the avalanche e^- contribute much less than the avalanche Xe^+. As in gas-filled proportional chambers, this is due to the fact that the avalanche occurs close to the anode and the avalanche electrons fall through relatively few equipotentials before they reach the anode.

In Fig. 8 we plot the ionization coefficient $\eta = \alpha/E$ as a function of E/ρ for liquid and gaseous xenon (where ρ is the density in g/cm^3). The curve drawn through the liquid-data points is the gas-data curve displaced to the left by a factor of 26.

The only published measurement of $\alpha(E)$ in xenon gas was that of Kruithof.[24] His experiment consisted of measuring the average current in a parallel-plate chamber as a function of electric field. Kruithofs' values of $\eta = \alpha/E$ (shown in Fig. 8) all lie on a very smooth curve, even though the data were taken at many different pressures, ranging from 0.28 to 165 Torr. We regard this as a very accurate demonstration of E/ρ scaling throughout the low-density region. We conclude that electrons in liquid Xenon do not avalanche as though they were in a gas having the density of liquid Xenon (3057 g/liter) but rather an effective density approximately 26 times smaller, assuming that η is a function of E/ρ only

One might speculate that the avalanche was occurring in some gas-liquid mixture near the surface of the wire, to account for the lack of density scaling. The existence of such a mixture might be suggested by the strong pressure dependence seen in the avalanche of ionization pulses in liquid argon.[9] However, the pulse height in liquid xenon, unlike that in liquid argon, is insensitive to pressure changes of the order of 1 to 2 atmospheres. It is difficult to see how a gas-liquid mixture could exist at the wire even at 1 atm external pressure, since the presence of 10^6 V/cm at the surface of the wire, along with the high gradient of the field, causes an additional pressure of approximately 1 atm on the liquid in the vicinity of the wire.

We find no evidence in the photopeak pulses for a second Townsend process. Photoelectrons liberated at the cathode by the prompt uv emission from excited Xe atoms would produce a second pulse delayed by 1.5 μsec, while electrons liberated at the cathode by the arrival of Xe^+ ions would produce a second pulse delayed by 1 sec. Such effects were not seen as multi-step pulses or as a background on the pulse-height analyzer. To investigate quantitatively the effect of possible second Townsend processes, we refit the data, assuming that for each ion pair generated in the avalanche, 3×10^{-4} new electrons were *promptly* liberated in the chamber and that these electrons initiated a fresh avalanche. This number was chosen so that the largest pulse heights shown in Fig. 4 would have about a 30% contribution from the second Townsend processes. If the secondary electrons originate near the cathode, then this assumption is pessimistic, as the second and subsequent avalanches would be delayed, producing an easily detectable multi-step pulse shape in contradiction with our observations. After

this fit, the only parameter that was changed from its value in Table II by more than 0.25 standard deviation was the first Townsend coefficient for 2×10^6 V/cm, and this was decreased by only 12% (1.8 standard deviations).

At voltages higher than those used in this experiment (as described in Section III), secondary processes dominate by producing spurious pulses of irregular shape and size. Such pulses were not seen at the lower voltage settings used in the data-taking phase of the experiment. Even had they been present, they would not have shifted the photopeak but would have added to the background on the pulse-height analyzer.

VI. RESULTS IN GASEOUS XENON

We have measured $\alpha(E)$ in pure gaseous xenon, using the 3.5- and 5.0-μ-diameter anode wires to check whether our technique (which uses detector pulses in a nonuniform field) would yield the same values as those of Kruithof[24] (who used direct current and a uniform field). Our measurement was performed by using the 5.9-keV x rays from an ^{55}Fe source and at a Xe gas pressure of 2.2 atm.[25] The resulting values of η for gaseous Xe fall slightly below those of Kruithof (see Fig. 8).

VII. DISCUSSION

In both liquid and gaseous Xe, the ionization coefficient η rises rapidly as a function of E, then levels off. We may view η as a direct measure of the efficiency for converting electron kinetic energy into ion pairs. If all the kinetic energy were used to create pairs with maximum efficiency, then η would be 0.0824 ion pairs/eV, corresponding to the ionization potential of 12.13 eV.

When an energetic electron (such as a 279-keV photoelectron) passes through Xe it loses energy through mechanisms other than ionization. As a result, the average ionization potential is higher:

21.9 eV/ion pair, corresponding to an η of 0.0457. We see from Fig. 8 that electrons heated to ionizing energies by an electric field are almost as efficient in creating ion pairs as are energetic electrons.

At present there is no theory of electron avalanche in dielectric liquids with which we can compare our experimental results. A few qualitative arguments, however, may serve to explain why electrons avalanche in liquid Xe more readily than in any other liquid studied to date. At very low electric fields, free electrons are in thermal equilibrium with the liquid and their drift velocity v_d is proportional to the electric field E. According to the qualitative theory of Shockley[26] and of Staub,[27] an increase in electron agitation energy (average instantaneous kinetic energy) is accompanied by a decrease in the electron mobility μ (defined as v_d/E). This behavior is seen in Fig. 9 for the liquified noble gasses [16,28] but not for the liquid hydrocarbons.[29] Electrons in polyatomic liquids suffer inelastic collisions as they excite vibrational and rotational states and as evidenced by their high mobility are apparently prevented from acquiring any significant agitation energy, even at fields of 10^5 V/cm. Of all the liquids for which we have measurements, liquid Xe has the highest ratio between its low-field and high-field mobilities. This high ratio is perhaps related to the ease of producing avalanche in liquid Xe.

Recently, Pisarev et al. have reported on a cylindrical proportional chamber filled with crystalline Xe.[30] Their chamber had a cathode diammeter of 6 mm, an anode diameter of 10 μ, and reached a gain of 150 at 5200 V. Using the values of $\alpha(E)$ measured in this experiment for liquid Xe and the positive ion (hole) mobility of 0.02 $cm^2\ V^{-1}\ sec^{-1}$ measured for

solid Xe,[16] we would predict a gain of 150 at 4100 V, in good agreement with the measured voltage. We conclude that the avalanche in solid Xe is very similar to that in liquid Xe.

Pisarev et. al., have also measured pulse height vs. voltage in the same chamber filled with gaseous xenon at pressures ranging from 1 to 50 atm.[31] Their solid-xenon data agree best with their gaseous-xenon data for 30 atm, showing that the required electric field for electron avalanche is similar in both gaseous xenon at a density of $\sim$240 g/liter and solid xenon at the much higher density of 3540 g/liter.

VIII. CONCLUSIONS

We find that the avalanche of free electrons in purified liquid Xe is adequately described by the same formalism that is used for the avalanche of electrons in gases. Although the ionization coefficient η (E/ρ) in liquid Xe has a shape similar to that measured in gaseous Xe, it is not the same function in the sense that strict "density scaling" does not apply. In gasses, η is a function of E/ρ over a large range of densities, but the function η (E/ρ) measured in gaseous Xe is valid in liquid Xe only when the electric field is scaled by an "effective density" of 117 g/liter rather than the true density of 3057 g/liter

ACKNOWLEDGMENTS

We are indebted to Joe Savignano, Tony Vuletich, and Buck Buckingham for their skill and patience in building and maintaining our equipment. We are grateful to Robert Flagg, Steven Louie, and Robbie Smits for assistance in data taking and to Leo Fallicov and Sherwood Parker for many helpful discussions. We thank Dane Anderberg for his excellent glass work and the Inorganic Materials Research Division of LBL for the use of their scanning electron microscope.

FOOTNOTES AND REFERENCES

* Work supported by the U.S. Atomic Energy Commission and the National Aeronautics and Space Administration.

1. N. Davidson and A. E. Larsh, Jr., Phys. Rev. 74, 220, (1948); 77, 706 (1950).
2. G. W. Hutchinson, Nature 162, 610 (1948).
3. M. S. Malkin and H. L. Schultz, Phys. Rev. 83, 1051 (1951).
4. John Marshall, Rev. Sci. Instr. 25, 232 (1954).
5. Due to the formation of a "bubble" around the electron in liquid He [L. Meyer and F. Reif, Phys. Rev. 110, 279 (1958) and R. L. Williams, Can. J. Phys. 35, 134 (1957),] and possibly in liquid Ne [L. Bruschi, G. Mazzi, and M. Santini, Phys. Rev. Letters 28, 1504 (1972)] the electron mobility in these liquids is considerably lower than in the liquids argon, krypton, and xenon.
6. D. W. Swan, Proc. Phys. Soc. 76, 36 (1960).
7. D. W. Swan, Proc. Phys. Soc. 83, 659 (1964).
8. L. W. Alvarez, Lawrence Radiation Laboratory Group A Physics Note 672, Nov. 26, 1968 (unpublished).
9. S. E. Derenzo, D. B. Smith, R. G. Smits, H. Zaklad, L. W. Alvarez, and R. A. Muller, Lawrence Radiation Laboratory Report UCRL-20118, National Accelerator Laboratory Summer Study Report SS-181, July 1970, Batavia, Illinois.
10. R. A. Muller, S. E. Derenzo, G. Smadja, D. B. Smith, R. G. Smits, H. Zaklad, and L. W. Alvarez, Phys. Rev. Letters 27, 532 (1971).
11. S. E. Derenzo, R. Flagg, S. G. Louie, F. G. Mariam, T. S. Mast, R. A. Muller, A. J. Schwemin, R. G. Smits, H. Zaklad, and L. W. Alvarez, Lawrence Berkeley Laboratory Report LBL-1321, in *Proceedings of the XVI International Conference on High Energy Physics, Chicago and Batavia, Illinois, September 1972*, Vol. 2, p. 388.
12. In liquid argon, the electron avalanche can occur only at places scattered sparsely along the wire (see Ref. 9). One consequence is that only a small fraction of incident particles initiate an avalanche, an effect also observed by E. A. Kushnirenko and A. G. Chilingarov (*Proceedings of the International Conference on High Energy Physics Instrumentation, Dubna, U.S.S.R.*, Vol. 1, p. 297, December 1971). In liquid xenon the avalanche occurs with ∿100% probability along the length of the wire.
13. Our fine tungsten wire was purchased from the following suppliers:
    a) 2.9 μ: Sigmund Cohn Corp. 121 South Columbus Avenue, Mount Vernon, N.Y. 10553.
    b) 3.5 μ: Philips Elmet Corp. Lewiston, Maine 04240 (no longer can supply wire below 5 μ diam).
    c) 5.0 μ: Sylvania Metals and Chemicals Towanda, Penn. 18848.
14. Supplied by Buckbee-Mears, 245 East 6th Street, St. Paul, Minn. 55101.
15. H. Zaklad, Lawrence Radiation Laboratory Report UCRL-20690, April 1971 (unpublished).
16. L. S. Miller, S. Howe, and W. E. Spear, Phys. Rev. 166, 871 (1968).
17. Yu. V. Kulikov, N. I. Molashkevich, and V. D. Ruabtsov, JINR P13-5403, Dubna (1970).
18. The effective range of electrons in liquid xenon was assumed to be similar to that measured in Aluminum by J. S. Marshall and A. G. Ward, Can J. Res. A15, 39 (1937).
19. G. Jaffe, Le Radium 10, 136 (1913). For a simpler discussion, see A. N. Gerritsen, Physica 14, 381 (1948).
20. Hans H. Staub, *Experimental Nuclear Physics*, Vol I, edited by E. Segrè (John Wiley, New York, 1952), p. 16.

21. H. Davis, S. Rice, and L. Meyer, J. Chem. Phys. 37, 947 (1962).

22. H. H. Staub, p. 35 of Ref. 20.

23. I. T. Myers, *Radiation Dosimetry*, Vol. 1, Ch. 7, Ionization, 2nd ed. (Academic Press, New York 1968).

24. A. A. Kruithof, Physica 7, 519 (1940).

25. S. G. S. Louie, Lawrence Berkeley Laboratory Group A Physics Note 765, 1972 (unpublished).

26. W. Shockley, Bell System Technical Journal 30, 990 (1951).

27. H. H. Staub, p. 6 of Ref. 20.

28. D. W. Swan, Proc. Phys. Soc. 83, 659 (1964).

29. W. F. Schmidt and A. O. Allen, J. Chem. Phys. 52, 4788 (1970).

30. A. F. Pisarev, V. F. Pisarev, and G. S. Revenko, Dubna Report JINR-P13-6449 (to be published in JETP).

31. A. F. Pisarev, V. F. Pisarev and G. S. Revenko, Dubna Report JINR-P13-6450 (to be published in JETP).

TABLE II.

Parameters resulting from the fit described in the text.

Quantity	Best Fit Value
Q_o' (2.9-μ run)	$(2.22\pm0.14)\times10^{-15}$C
Q_o' (3.5-μ run)	$(1.86\pm0.10)\times10^{-15}$C
Q_o' (5.0-μ run)	$(1.96\pm0.14)\times10^{-15}$C
K	$98\ ^{+12}_{-10}$ V/cm
λ	$0\ ^{+10}_{-0}$ V/cm^2
α (400 kV/cm)	$470\ ^{+600}_{-470}$ cm^{-1}
α (600 kV/cm)	8050 ± 3500 cm^{-1}
α (800 kV/cm)	$2550\ ^{+7000}_{-2550}$ cm^{-1}
α (1000 kV/cm)	$8300\ ^{+3400}_{-4700}$ cm^{-1}
α (1200 kV/cm)	15000 ± 6000 cm^{-1}
α (1400 kV/cm)	27500 ± 6000 cm^{-1}
α (1600 kV/cm)	33500 ± 4500 cm^{-1}
α (1800 kV/cm)	38400 ± 4500 cm^{-1}
α (2000 kV/cm)	44700 ± 2600 cm^{-1}

FIGURE CAPTIONS

Fig. 1. Liquid xenon single-wire proportional chamber. Cathode is 8 mm diameter, formed by depositing a conductive coating of SnO onto the inside glass wall. Central anode wires of 2.9-, 3.5-, and 5.0-μ-diameter tungsten were used. Chamber was connected directly to a charge amplifier.

FIG. 2. Scanning electron micrographs of the tungsten anode wires used in this experiment. The 2000 mesh per inch Buckbee-Meers screen (used for calibration) may be seen beneath the 5-μ wire.

FIG. 3. Pulse-height spectrum from a collimated ^{203}Hg source in chamber of Fig. 1 filled with liquid xenon, using a 3.5-μ anode at 2400 V, showing 68-keV photopeak, 279-keV Compton edge, and 279-keV photopeak. Gain in the liquid was 10 and the field at the anode surface was 1.8×10^6 V/cm.

FIG. 4. Pulse height of 279-keV photopeak vs voltage for 2.9-, 3.5-, and 5.0-μ-diameter anode wires.

FIG. 5. Data of Fig. 4 shown with best fit curves. See test for details.

FIG. 6. Calculated pulse size for a 2.9-μ anode as a function of photoelectron position for a series of applied voltages. Calculation based on best fit parameters shown in Table II.

FIG. 7. Calculated curves comparing the size of the avalanche with the size of the e^- and Xe^+ ion contributions to the observed pulse. All curves are normalized to one initial e^- and based on the best fit $\alpha(E)$ function shown in Table II. [See Eqs. (5.1) to (5.3) and associated text for further details.] Solid lines: charge of e^- (and Xe^+) produced in the avalanche. Dot-dashed lines: charge induced by the avalanche Xe^+ ions in

the first 2 μsec. Dotted lines: charge induced by the avalanche electrons.

FIG. 8. Ionization coefficient vs the ratio of electric field to density for gaseous xenon (squares, Ref. 24; circles, this experiment) and for liquid xenon (circles, this experiment). The curve drawn through the liquid-data points is the gas data curve of Ref. 24 displaced to the left by a factor of 26.

FIG. 9. Electron drift velocities observed for various liquids as a function of electric field. Liquified noble gases at their normal boiling points (Refs. 5 and 16). Liquid hydrocarbons at 23°C (Ref. 29). Solid lines: observed data; dashed lines: linear extrapolations.

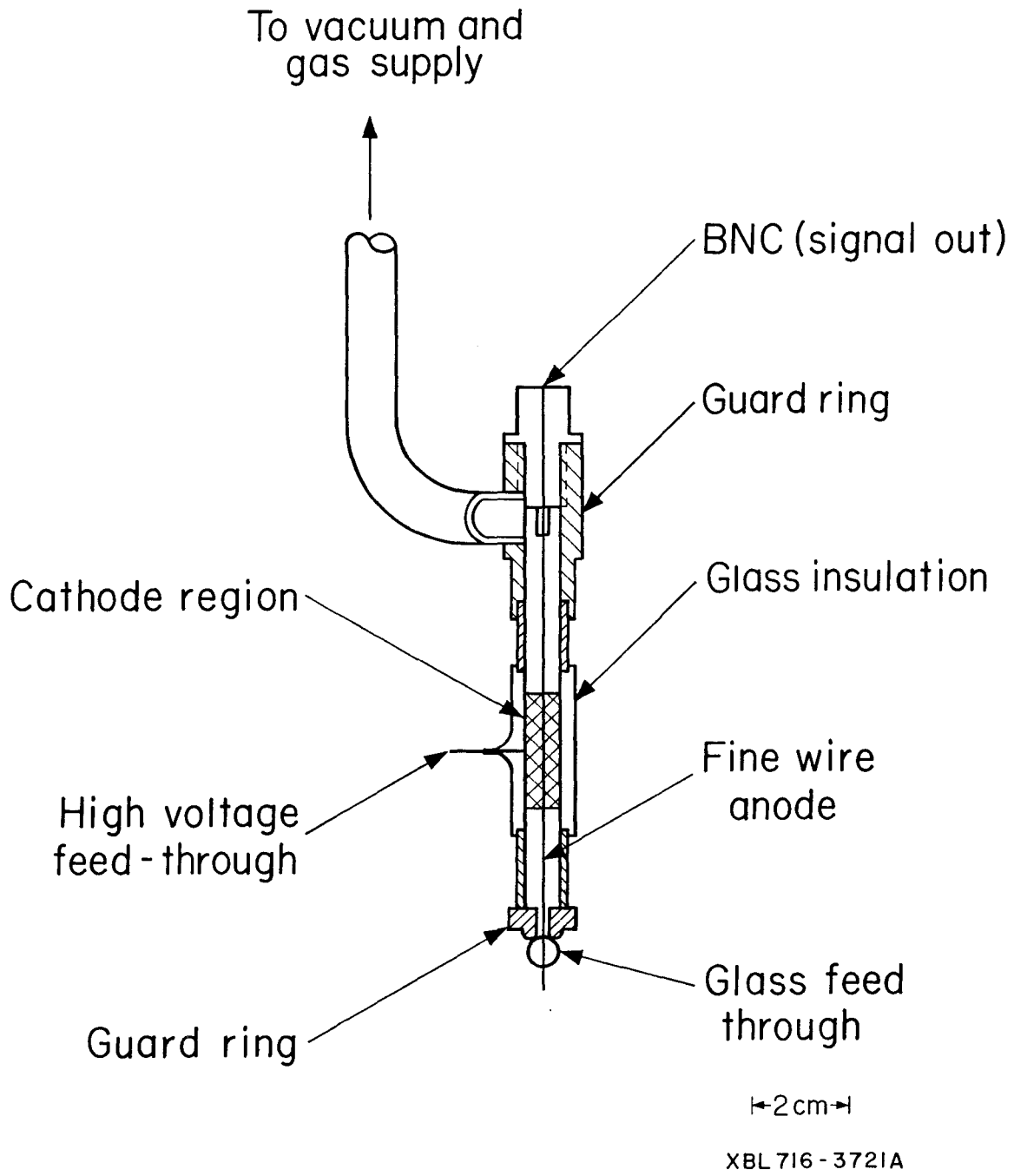
To vacuum and
gas supply
BNC (signal out)
Guard ring
Glass insulation
Cathode region
Fine wire
anode
High voltage
feed-through
Glass feed
through
Guard ring
2cm
XBL 716-3721A

Fig. 1

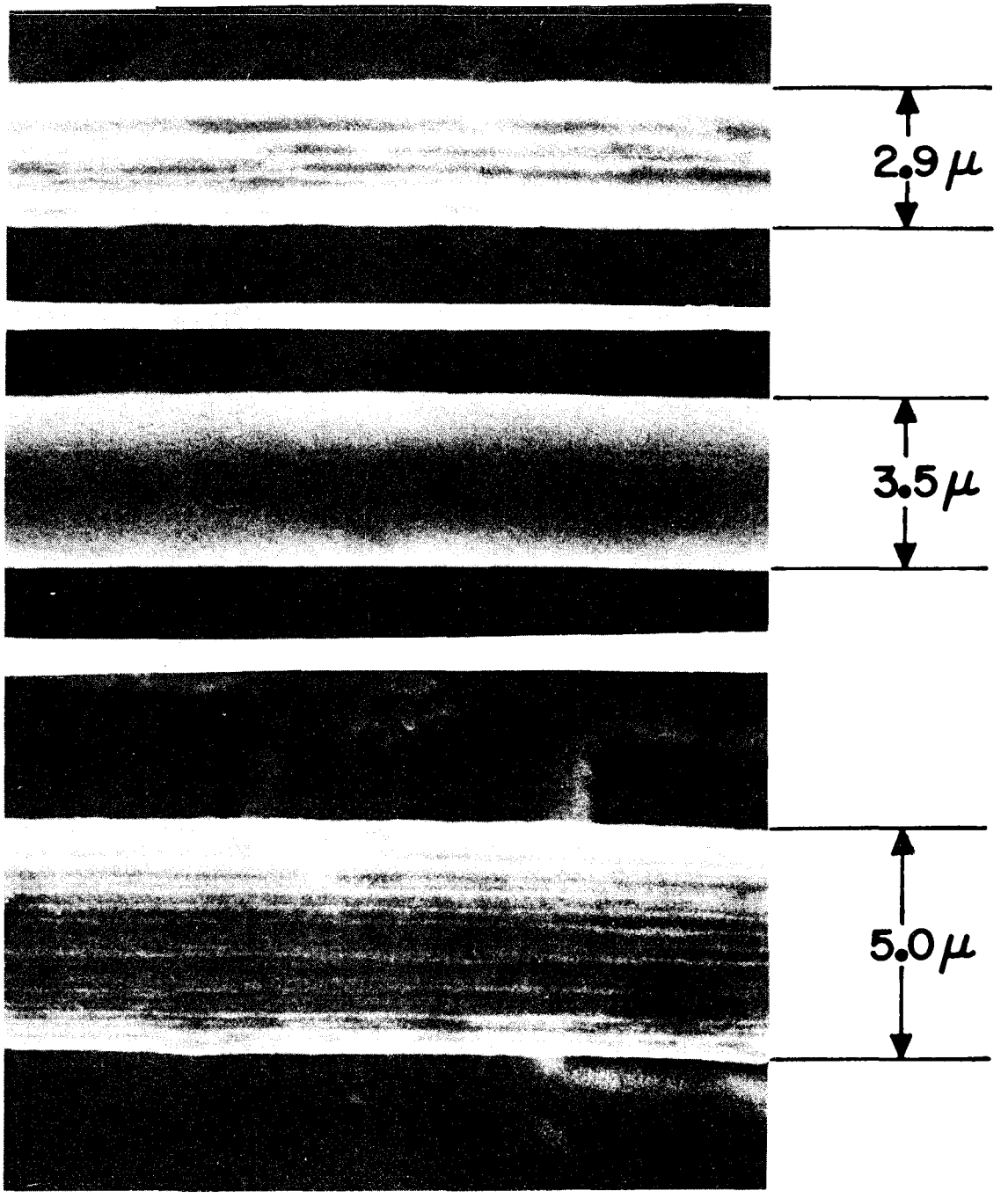

XBB 728-4278

Fig. 2

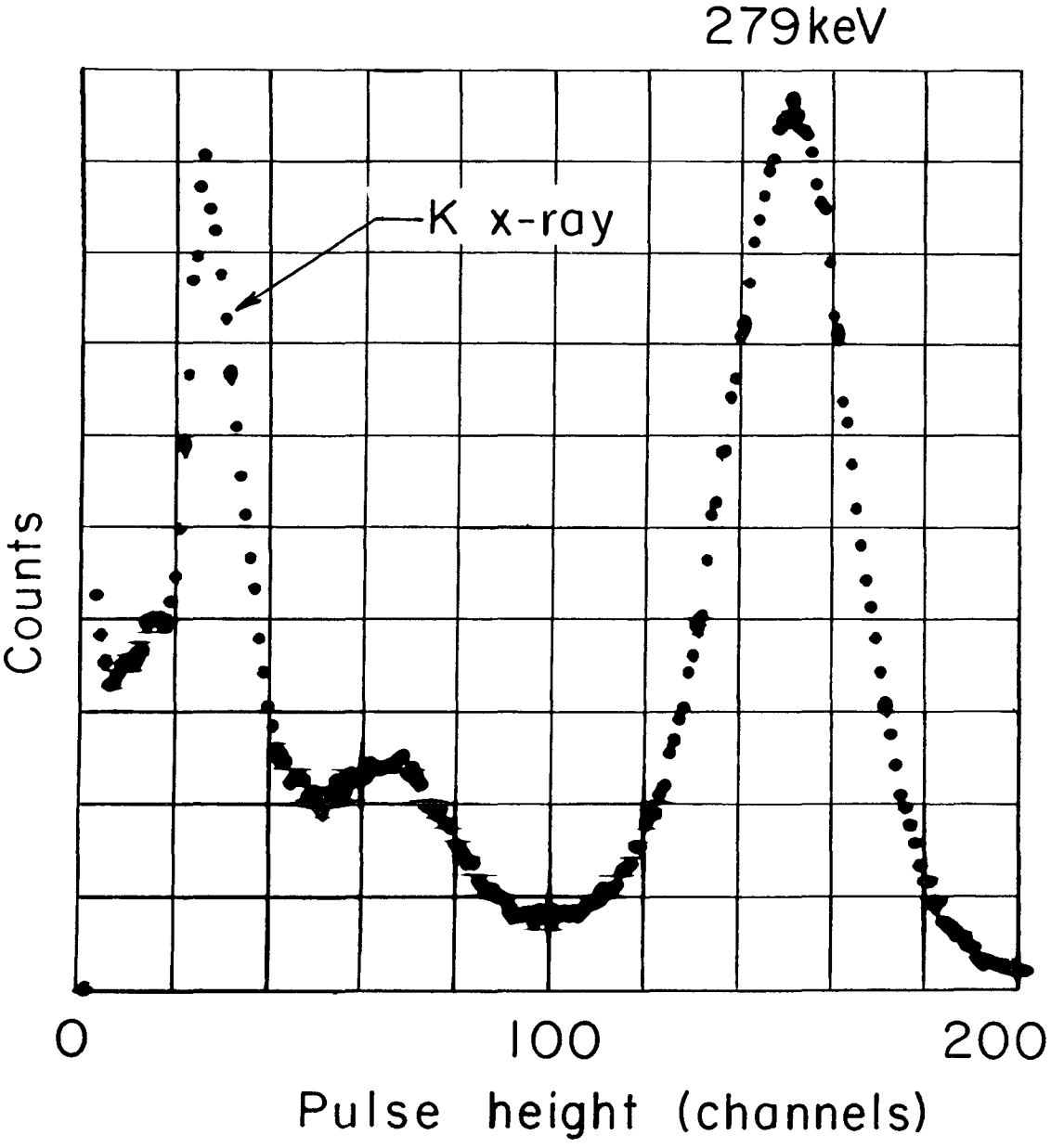

XBL722-2248

Fig. 3

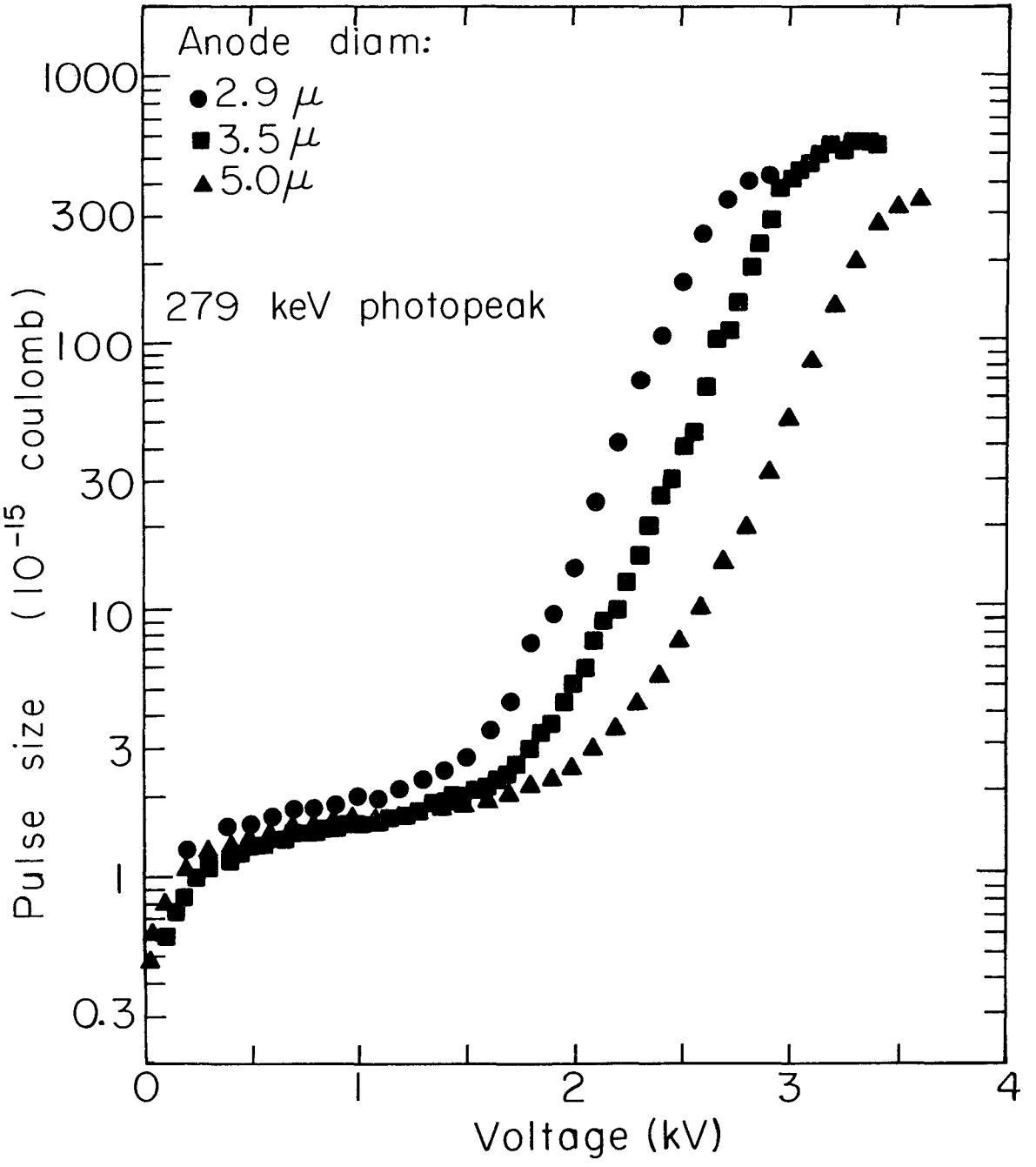

XBL734-2639

Fig. 4

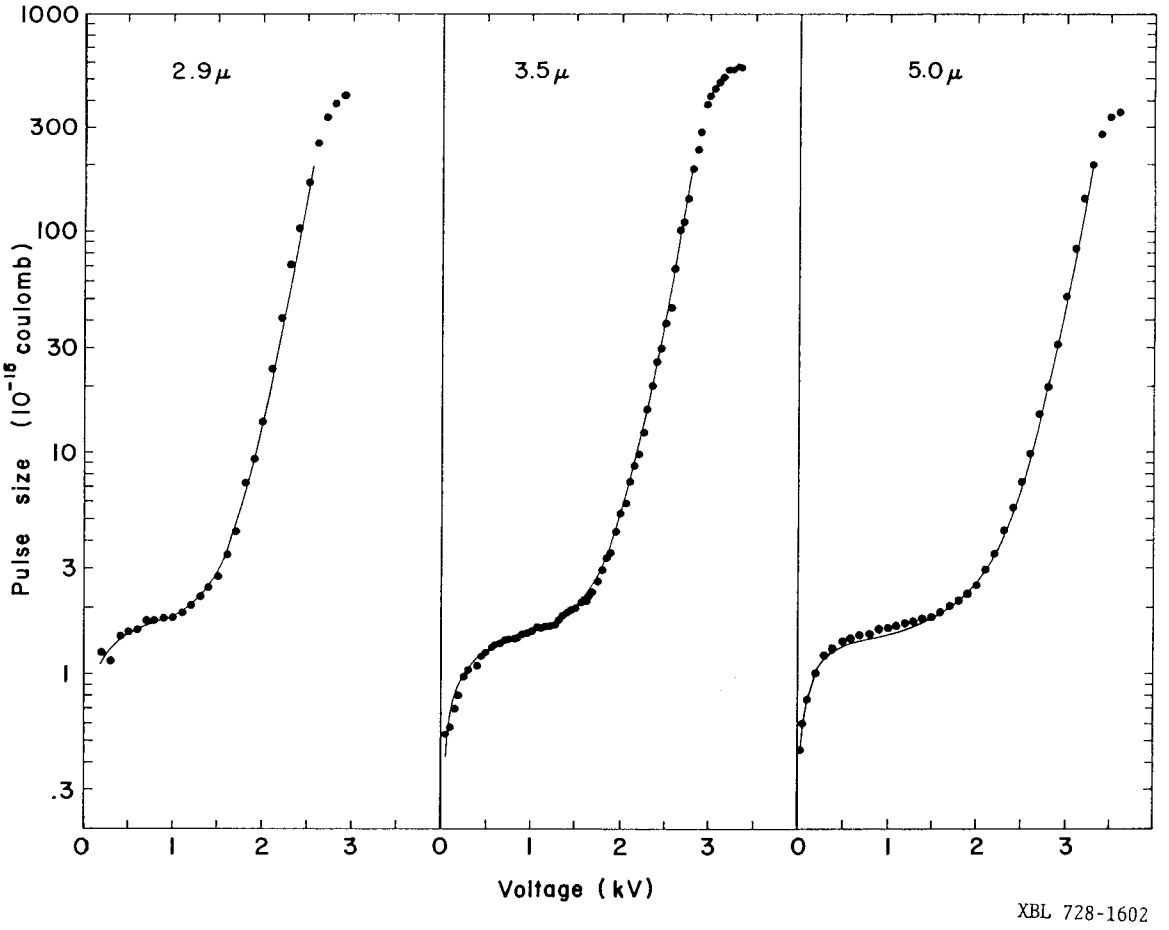
2.9μ
3.5μ
5.0μ
Pulse size (10^{-15} coulomb)
1000
300
100
30
10
3
1
.3
0
1
2
3
Voltage (kV)
XBL 728-1602

Fig. 5

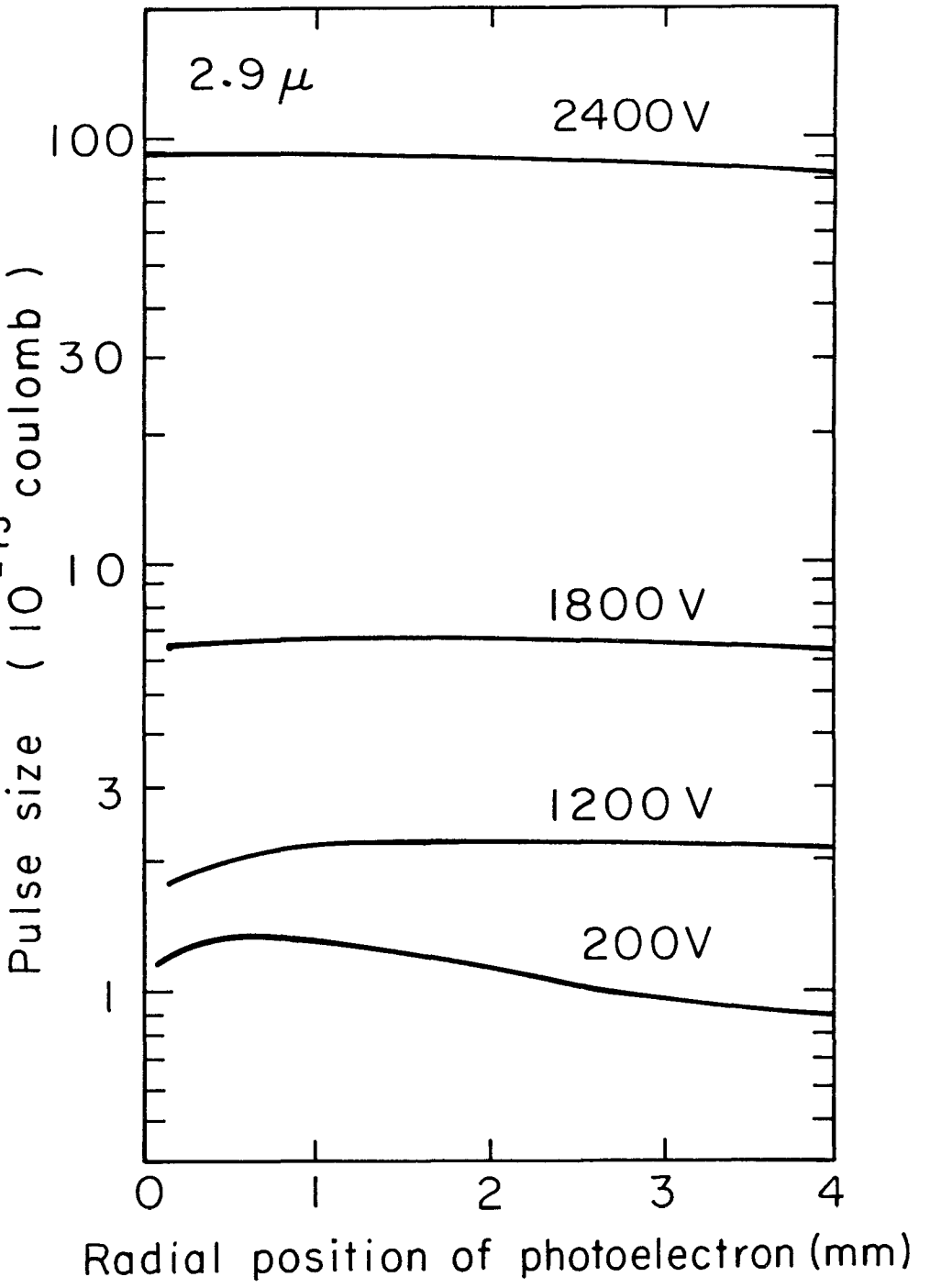

XBL734-2621

Fig. 6

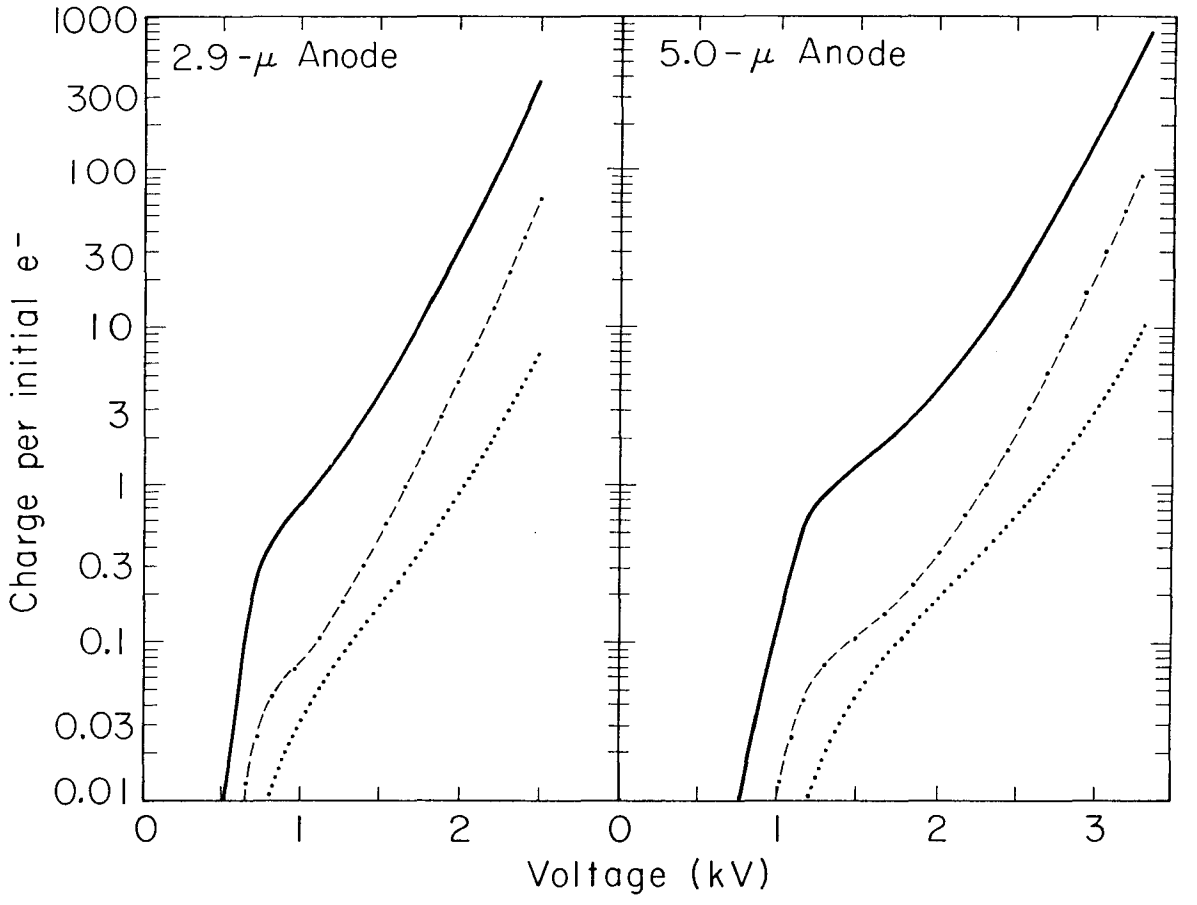

XBL734-2620

Fig. 7

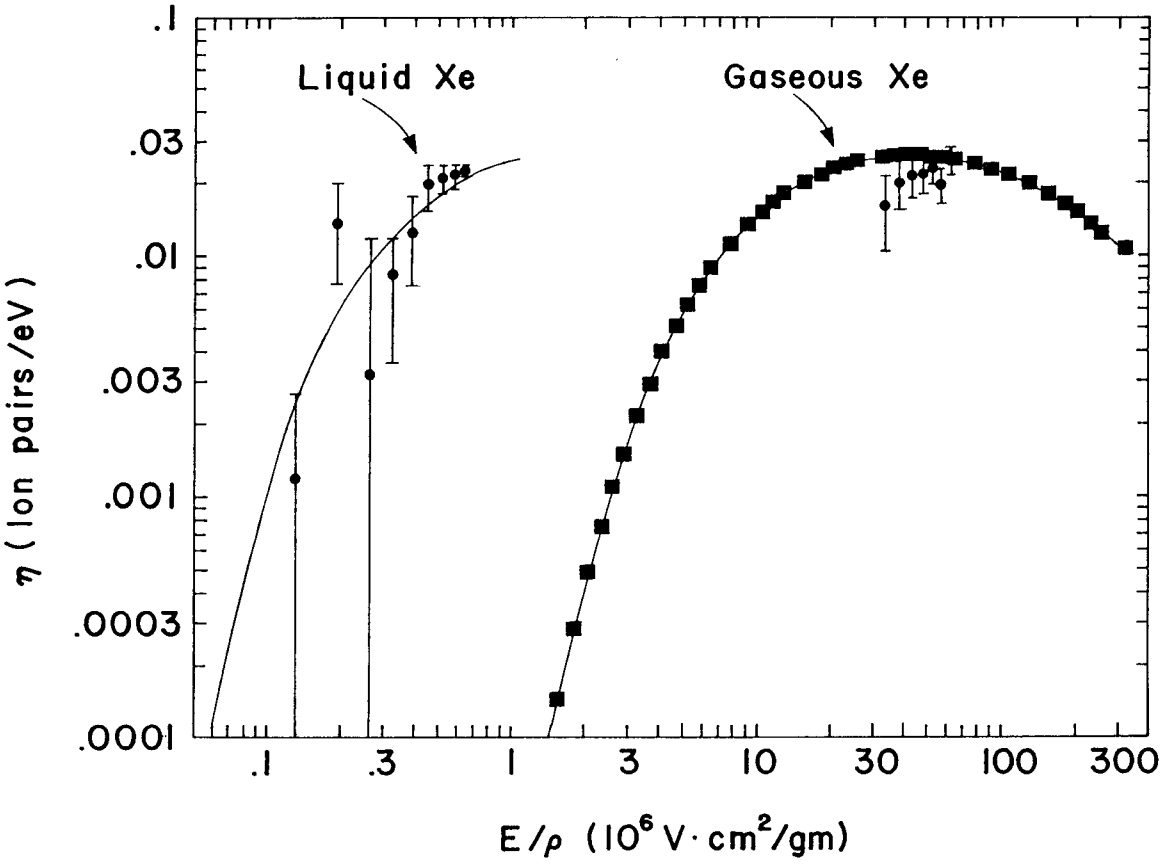
Liquid Xe
Gaseous Xe
η (Ion pairs /eV)
.1
.03
.01
.003
.001
.0003
.0001
.1
.3
1
3
10
30
100
300
E/ρ (10⁶ V·cm²/gm)
XBL 728-1601

Fig. 8

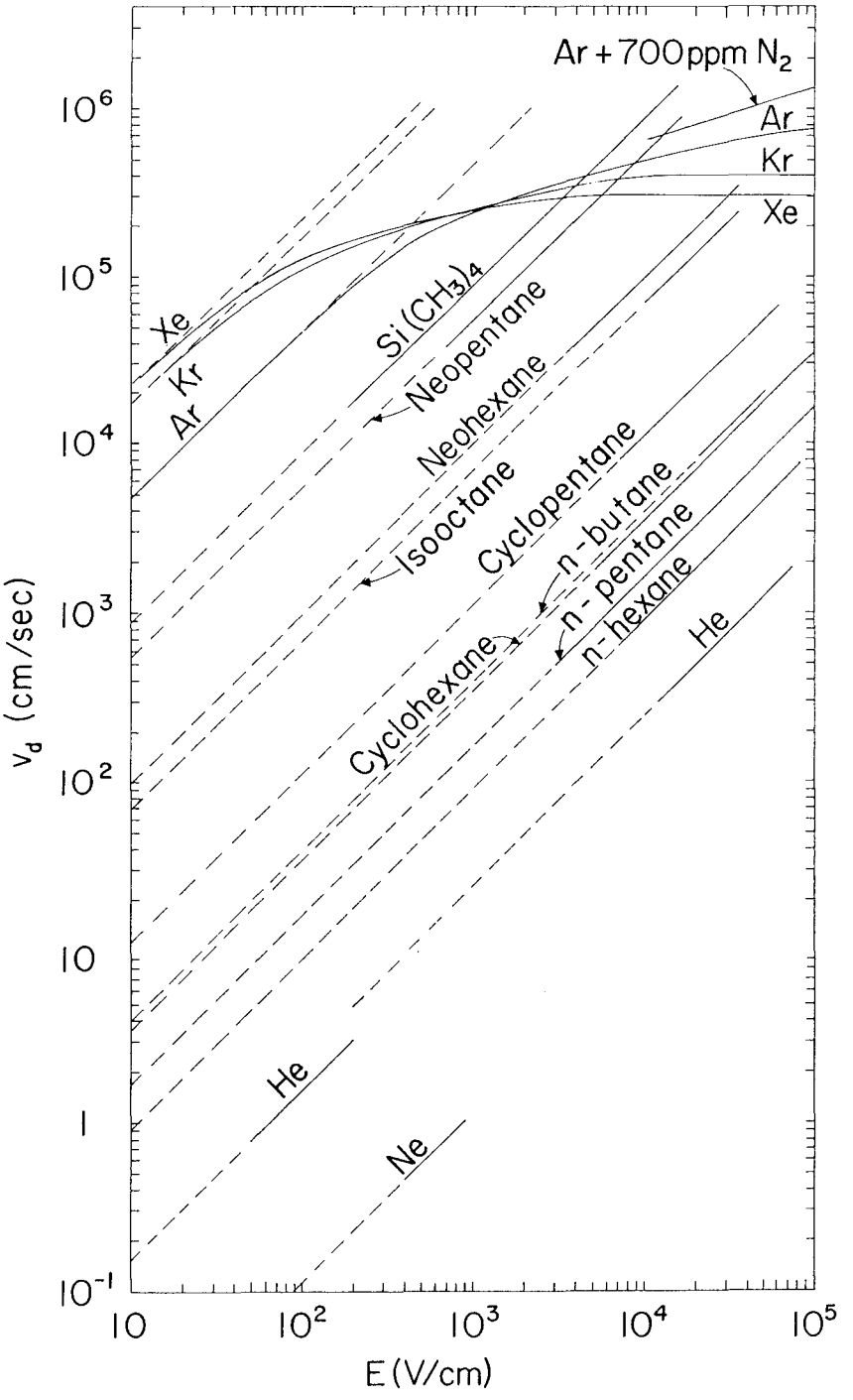

XBL 719-4252A

Fig. 9